Functional immune characterization of HIV-associated non-small cell lung cancer.

Journal:	*Annals of Oncology*
Manuscript ID	ANNONC-2017-2443.R2
Manuscript Type:	Letter to the Editor
Date Submitted by the Author:	27-Mar-2018
Complete List of Authors:	Pinato, David James; Imperial College, Surgery and Cancer Kythreotou, Anthousa; Imperial College, Surgery and Cancer Mauri, Francesco; Imperial College London, Histopathology Suardi, Elisa; Chelsea and Westminster Hospital NHS Foundation Trust, National Centre for HIV Malignancy Allara, Elias; Università degli Studi di Torino, Public Health Shiner, Robert; Imperial College, Surgery and Cancer Akarca, Ayse; University College London Cancer Institute, Department of Oncology Trivedi, Pritesh; Imperial College, Department of Histopathology Gupta, Nandita; Imperial College, Histopathology Dalla Pria, Alessia; Chelsea and Westminster Hospital NHS Foundation Trust, National Centre for HIV Malignancy Marafioti, Teresa; University College Hospital London, Cellular Pathology; Oliveri, Paola; University College London Research Department of Genetics Evolution and Environment, Genetics Evolution and Environment Newsom-Davis, Tom; Chelsea and Westminster Hospital, Oncology and HIV Medicine Bower, Mark; Imperial College, Oncology
Keywords:	PD-L1, PD-L2, NSCLC, HIV, PD-1, lung cancer
Abstract:	N/A

Functional immune characterization of HIV-associated non-small cell lung cancer.

D.J. Pinato[1,2], A. Kythreotou[1], F. A. Mauri[1,3], E. Suardi[2], E. Allara[1,4], R. Shiner[5], A. U. Akarca[6], P. Trivedi[3], N. Gupta[3], A. D. Pria[2], T. Marafioti[6], P. Oliveri[7], T. Newsom-Davis[4], M. Bower[4]

1. Department of Surgery & Cancer, Imperial College London, Hammersmith Hospital, Du Cane Road, W120HS London, UK.

2. National Centre for HIV Malignancies, Chelsea & Westminster Hospital, SW10 9NH London (UK).

3. Department of Histopathology, Imperial College London, Hammersmith Hospital, Du Cane Road, W120HS London, UK.

4. NIHR Blood and Transplant Research Unit, Department of Public Health and Primary Care, University of Cambridge, UK

5. National Heart and Lung Division, Imperial College London (UK)

6. Department of Histopathology, University College London, 4th Floor Rockefeller Building, 21 University Street, London WC1E 6DE.

7. Department of Genetics, Evolution and Environment & Cell and Developmental Biology University College London Room 432, Darwin Building Gower Street, London, WC1E 6BT, UK

Word Count: 500 **Tables:** 0 **Figures:** 1

Running Head: *Immune characterisation of HIV-associated lung cancer*

To whom correspondence should be addressed:

Professor Mark Bower

E-mail: m.bower@imperial.ac.uk

Letter to the Editor.

Dear Editor,

In the combined anti-retroviral therapy (cART) era, non-small cell lung cancer (NSCLC) is a highly incident cause of morbidity and mortality in people living with HIV (PLHIV)[1]. The immune-pathogenesis of NSCLC and HIV infection both rely on programmed-death 1 (PD-1) receptor-ligand interaction as a mechanism to induce T-cell exhaustion. To date, PLHIV have been excluded from clinical trials of immune-checkpoint inhibitors (ICPI), on the presumption that anti-tumour immunity might be compromised by HIV infection. To verify this, we evaluated the clinico-pathologic significance of PD-ligands expression in a consecutive series of 221 archival NSCLC samples, 24 of which were HIV-associated (**Table S1**).

Most patients with HIV-associated NSCLC were active smokers (*n*=18, 75%; median 40 packs/year, IQR 48), established on cART (*n*=22, 92%) for a median duration of 9.7 years (IQR 7.1) with CD4 counts >250 cells/mm^3 (*n=19*, 79%) and suppressed HIV RNA (*n*=20, 80%). Molecular profiling data (*n*=12/24) revealed two EGFR mutation carriers. Tissue-microarray sections underwent PD-L1, PD-L2 immunostaining and multiplex immunohistochemistry (*n*=21) for PD-1, CD4, CD8 and CD68 (**Figures 1A-D, Supplementary Materials**). Prevalence of PD-L1 positivity was

45% in tumour (*n*=11/24) and 8% (*n*=2/24) in tumour-infiltrating cells, whereas tumoural PD-L2 positivity was found in 33% (*n*=8/24) (**Figure S1)**. Following 2:1 case-control matching for age, gender, grade, stage and histotype (*n*=66), PD-L1 (12/23 vs 14/43, p=0.12) and PD-L2 expression (9/23 vs 25/45, p=0.20) were unrelated to the presence and severity of HIV-related immune dysfunction as indicated by nadir CD4 counts (p=1.0, p=0.8), HIV RNA levels (p=0.14, p=0.24), duration of HIV infection and cART (p>0.05) suggesting independence between anti-viral and anti-tumour immune-tolerogenesis. In keeping with this view, we documented a positive correlation between PD-L1 expression and density of tumour-infiltrating (TIL) (**Figure 1A-F**) but not peripherally circulating lymphocytes (**Figure 1G-H**), highlighting polarization of the tumour microenviroment to a type-1 response[2]. In type-1 or PD-L1$^+$/TIL$^+$ tumours, TILs are chemo-attracted to malignant cells and turned off by PD-L1 engagement. Type-1 tumours are generally sensitive to single-agent PD-1/PD-L1-targeted checkpoint blockade, due to the presence of an immune-reactive microenvironment[3].

In an exploratory targeted transcriptomic analysis of 5 HIV-positive cases and 3 stage/histotype-matched controls using the NanoString PanCancer-Immune panel (NanoString Technologies, Seattle, USA), we demonstrated enrichment of transcripts involved in chemotaxis (CCL18), antigen presentation (HLA-A, HLA-DRA), cytotoxic T-cell (LAMP-1) and macrophage activation (SPP1, **Figure 1I-L**) in HIV-associated NSCLC, consistent with previous studies[4]. Whilst not exhaustive and limited by sample size, our findings challenge the conception that well-controlled HIV infection may negatively influence cancer-specific immune dysfunction by preliminarily demonstrating the presence of an immune-reactive microenvironment in HIV-associated

NSCLC (**Figure S2-3, Table S2-3**). This concept should be further explored by comparing normal and neoplastic lung tissues in prospective studies.

As accumulating evidence shows PD-1/PD-L1-targeted ICPI to be safe and capable of enhancing HIV-specific immunity[5] without unexpected toxicity, taken together, our data suggest that HIV-associated NSCLC may be equally reactive to ICPI. Whilst preliminary in nature and warranting validation in larger patient cohorts treated with ICPI, our study supports an immunobiologic rationale for the development of PD-1/PD-L1-targeted ICPI in HIV-associated NSCLC.

References.

1. Bower M, Powles T, Nelson M et al. HIV-related lung cancer in the era of highly active antiretroviral therapy. AIDS 2003; 17: 371-375.

2. Teng MW, Ngiow SF, Ribas A, Smyth MJ. Classifying Cancers Based on T-cell Infiltration and PD-L1. Cancer Res 2015; 75: 2139-2145.

3. Taube JM, Klein A, Brahmer JR et al. Association of PD-1, PD-1 ligands, and other features of the tumor immune microenvironment with response to anti-PD-1 therapy. Clin Cancer Res 2014; 20: 5064-5074.

4. Domblides C, Antoine M, Hamard C et al. Non-small cell lung cancer from HIV-infected patients expressed PD-L1 with marked inflammatory infiltrates. AIDS 2017.

5. Guihot A, Marcelin AG, Massiani MA et al. Drastic decrease of the HIV reservoir in a patient treated with nivolumab for lung cancer. Ann Oncol 2017.

Figure Legends.

Figure 1. Panel A-D. Representative sections of HIV-associated NSCLC co-immunostained for CD8 (red chromogen), CD4 (brown chromogen), PD-1 (blue chromogen) and CD68 (green chromogen) illustrating CD4/CD8 enrichment in PD-L1-positive HIV-associated NSCLC (**Panels A-C**) compared to PD-L1-negative counterparts (**Panels B-D**). **Panels E-F** Histograms of multiplex immunohistochemistry data illustrating the relationship between the CD4 and CD8-positive immune infiltrate expressed as number of immunopositive cells per high power field (HPF) according to tumour cell PD-L1 (**Panel E**) and PD-L2 expression status (**Panel F**) in HIV-associated NSCLC (*n*=21). **Panels G-H** Peripheral blood immunophenotyping illustrates the relationship between peripheral CD4, CD8, CD19 and CD56-positive cell counts categorized according to tumoural PD-L1 (**Panel G**) and PD-L2 expression status (**Panel H**) in HIV-associated NSCLC (*n*=24). Medians and interquartile ranges are reported. **Panel I:** Volcano plot of differentially-regulated genes identified by Nanostring analysis. The Benjamini-Hockberg p-values are correlated to fold-changes in transcripts identified in HIV-positive NSCLC (*n*=5) versus HIV-negative controls (*n*=3). Transcripts achieving statistical significance (FDR q-value of 5%) are highlighted by the presence of the corresponding gene name. **Panel L.** Heat map profile of the 12 transcripts that are differentially regulated in HIV-associated NSCLC compared to controls. Expression levels are shown as log transformed values of normalized counts (ln2).

Conflict of interest: None declared.

Acknowledgements.

The authors would like to acknowledge the Imperial College Healthcare NHS Trust Tissue Bank for having supported the study.

Funding

DJP is supported by grant funding from the National Institute for Health Research (NIHR), the Imperial Biomedical Research Centre and the Academy of Medical Sciences (AMS Grant ID SGL013/1021). The AMS Starter Grant is jointly funded by the AMS, Wellcome Trust, Medical Research Council, British Heart Foundation, Arthritis Research UK, the Royal College of Physicians and Diabetes UK.

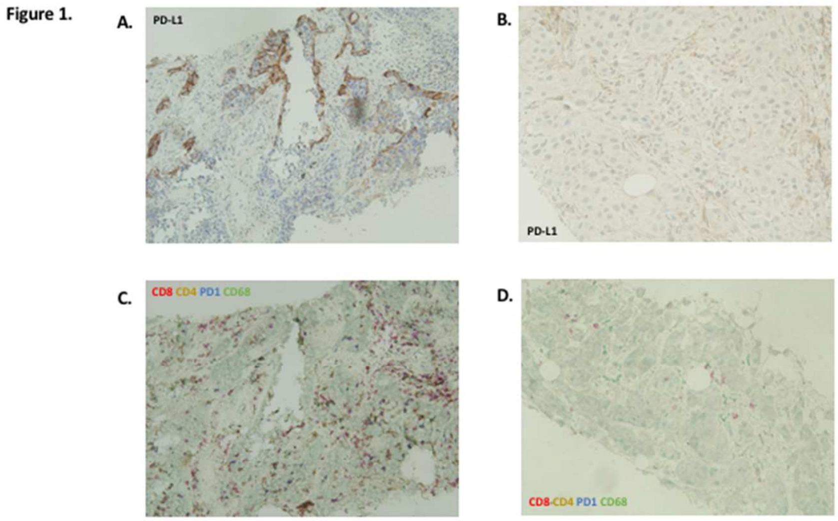

Fig 1abcd

338x190mm (54 x 54 DPI)

Figure 1.

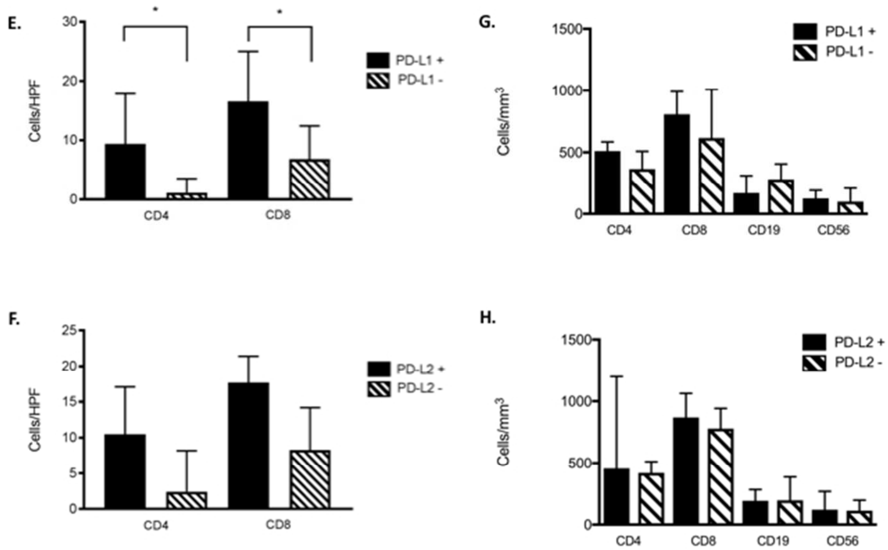

fig 1efgh

338x190mm (54 x 54 DPI)

Figure 1.

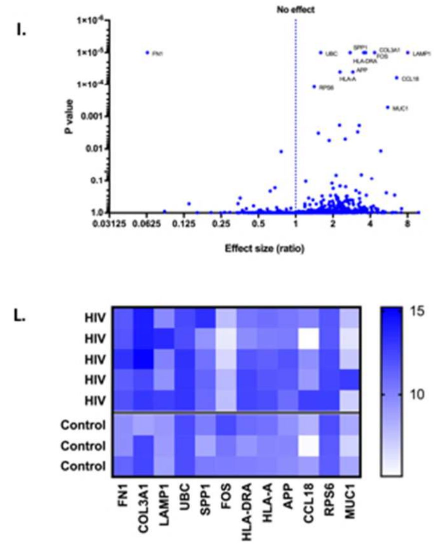

fig 1il

338x190mm (54 x 54 DPI)

Supplementary Materials and Methods.

Functional immune characterization of HIV-associated non-small cell lung cancer.

David J. Pinato et al.

Patient Samples.

From a series of 256 patients diagnosed with NSCLC (2001-2016) within Imperial College London affiliated hospitals, we identified a subset of 36 patients with NSCLC on a background of HIV whose oncological and HIV care was coordinated within the National Centre for HIV malignancies at the Chelsea and Westminster Hospital. We excluded 36 patients due to insufficient tissue, leaving 221 available for analysis: 24 HIV-positive and 197 HIV-negative. Clinico-pathologic variables including overall survival (OS) were derived from a prospectively maintained dataset. The study was approved by the Imperial College Tissue Bank (R16005), which issued a waiver of consent due to the retrospective nature of the study. Study related procedures were conducted in accordance to the Declaration of Helsinki.

Patients and Tumour Characteristics.

Our study population consisted of 234 patients, out of whom 218 (93%) had full immunohistochemical data for PD-L1 and PD-L2 expression, leaving a total of 24 HIV-positive and 194 HIV-negative individuals. The clinico-pathologic features of our patient population are described in **Table S1**. Patients with HIV-associated NSCLC were predominantly of male gender (n=21, 87%). The most prevalent risk factor for HIV infection was MSM sexual transmission (n=15, 63%). The majority of patients (n=19, 79%) had peripheral CD4 counts >250 cells/mm^3 and a suppressed HIV viral load (n=20, 80%). Most patients were established on anti-retroviral therapy (ARVs) at the time of LC diagnosis (n=22, 92%) with a median duration of treatment of 9.7 years (IQR

7.1 years) and a median interval between diagnosis of HIV and NSCLC of 16 years (IQR 8.2 years). A total of 6 patients (25%) had a history of at least one previous respiratory opportunistic infection (OI) including recurrent bacterial (n=3), mycobacterial (n=3), fungal OIs (n=2) and Pneumocystis pneumonia (n=2). According to the U.S. Centers for Disease Control and Prevention (CDC) classification system, the majority of patients satisfied group C criteria (n=14). Overall, 8 patients (33%) were treated radically for their NSCLC either by surgery (n=7, 29%) or radical radiotherapy (n=1, 4%), whereas 14 (58%) received palliative treatments including chemotherapy (n=10, 42%), targeted therapies (n=3, 12%) and palliative radiotherapy (n=8, 33%). Two patients (8%) received best supportive care only. At the time of censoring in June 2017, 19 patients (80%) had died and the median overall survival (OS) was 9.5 months (95%CI 4.8-14.2).

<u>Tissue microarray (TMA) construction and immunohistochemistry (IHC).</u>

Following review of haematoxylin and eosin (H&E) slides to confirm salient histopathologic features including TNM stage (7th edition)[1], one mm tissue cores from archival paraffin-embedded specimens were sampled in triplicate to prepare TMA blocks using an MTA-1 Manual Tissue Microarrayer (Beecher Instruments, USA)[2]. Biopsy samples lacking enough tissue for re-embedding in a TMA blocks were processed on full-face sections.

IHC staining was performed on 5µm sections using the Leica Bond RX stainer (Leica, Buffalo, IL) using a pre-specified protocol[3]. The primary antibodies anti-PD-L1 (Clone

E1L3N; Cell Signalling Cat. Nr. 13684), anti-PD-L2 (Sigma Aldrich, Cat. Nr. 3500395) were incubated overnight at the concentration 1:100 and 1:300, respectively. A secondary antibody was incubated for 1 hour at room temperature and then processed using the Polymer-HRP Kit (BioGenex, San Ramon CA, US) with development in diaminobenzidine and Mayer's Haematoxylin counterstaining. For each experiment, positive (de-identified tonsil) and negative controls (omission of primary antibody on tonsil sections) were processed in parallel. HIV-associated NSCLC samples (n=21) underwent multi-colour immune cell phenotyping for PD-1 (clone NAT 105/E3), CD4 (Spring Biosciences, clone SP35), CD8 (clone SP239) and CD68 (clone SP251) based on a previously optimised protocol[4]. Specificity of immunostaining was confirmed by a haematopathologist with expertise in multiplex IHC (TM) and immune cell density was quantified on a total of 10 high-power fields (HPF) per sample.

IHC expression of PD ligands was evaluated independently by 2 lung histopathologists (FAM, NG) using a semi-quantitative immuno-histoscore (IHS) derived by multiplying percentage of immunopositive cells by signal intensity[2]. Continuous IHS ranging from 0-300 were categorised around the median of the distribution for clinicopathologic correlation. Tumour cell or peri-tumoural stromal expression was considered specific only if membranous or concomitant membranous and cytoplasmic staining were present.

NanoString Immune profiling.

We performed H&E-guided manual microdissection of target tumour tissue in a subset of 10 samples (6 cases and 4 stage and histotype-matched controls) and extracted total RNA on 2-4 5 μM-thick tissue sections using the Qiagen RNAeasy FFPE kit (Qiagen, Venlo, NL, Cat Nr. 73504) according to the manufacturer's instructions. We performed targeted transcriptomic profiling using the NanoString PanCancer Immune panel on an nCounter® Analysis System (NanoString Technologies, Seattle, USA). Hybridization reactions were performed according to the manufacturer's instructions. The PanCancer Immune CodeSet (NanoString Technologies) contains a biotinylated capture probe for 770 target genes and 40 housekeeping genes. For each sample 200 ng of total RNA were hybridised to multi-colour-tagged reporter probes for 18 hours at 65°C and processed on an automated nCounter® Prep Station. Following purification and immobilisation of hybridized samples, target mRNA quantification was performed on an nCounter® Digital Analyzer, counting 600 fields of view per reaction. Quantified expression data were analyzed using the nSolver analysis software version 4.0. The resulting counts were normalized to the average counts for all control spikes in each sample and subsequently normalized using the geometric mean of the housekeeping genes. Samples flagged for high normalisation values or with quality control standards falling outside default settings were examined carefully and a total of 2 samples (1 HIV, 1 control) were excluded, leaving 8 samples (5 HIV and 3 controls) for final analysis.

Statistical analysis.

Patients' characteristics were presented as means or medians as appropriate. Pearson chi-square or Fisher's exact tests were used for analysis of proportions. All statistical analyses were performed using SPSS version 21.0 (IBM Inc., Chicago, IL, USA) and GraphPad PRISM (GraphPad software inc., La Jolla, CA, USA) with all estimates being reported with corresponding 95% confidence intervals and a two-tailed level of significance of $p<0.05$. Differential expression of genes of interest was determined using the false discovery rate method (FDR) of Benjamini and Hochberg, with pre-defined q-value of 5%.

Supplementary References.

1. Sobin LH, Gospodarowicz MK, Wittekind C. TNM Classification of Malignant Tumours, 7th Edition. Wiley-Blackwell, 2009.

2. Pinato DJ, Tan TM, Toussi ST, Ramachandran R, Martin N, Meeran K, et al. An expression signature of the angiogenic response in gastrointestinal neuroendocrine tumours: correlation with tumour phenotype and survival outcomes. Br J Cancer 2014; 110:115-22.

3. Pinato DJ, Shiner RJ, White SD, Black JR, Trivedi P, Stebbing J, et al. Intra-tumoral heterogeneity in the expression of programmed-death (PD) ligands in isogeneic primary and metastatic lung cancer: Implications for immunotherapy. Oncoimmunology 2016; 5:e1213934.

4. Marafioti T, Jones M, Facchetti F, Diss TC, Du MQ, Isaacson PG, et al. Phenotype and genotype of interfollicular large B cells, a subpopulation of lymphocytes often with dendritic morphology. Blood 2003; 102:2868-76.

Supplementary Results.

Functional immune characterization of HIV-associated non-small cell lung cancer.

David J. Pinato et al.

- Figure S1 Pages 1-3
- Figure S2 Page 4
- Figure S3 Page 5
- Table S1 Pages 6-7
- Table S2 Page 8
- Table S3 Page 9

Figure S1.

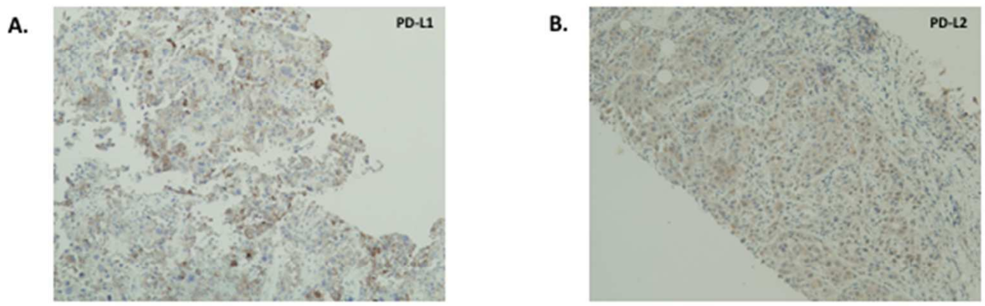

Panels A-B. Representative sections illustrating PD-L1 (**A**) and PD-L2 expression (**B**) in HIV-associated NSCLC.

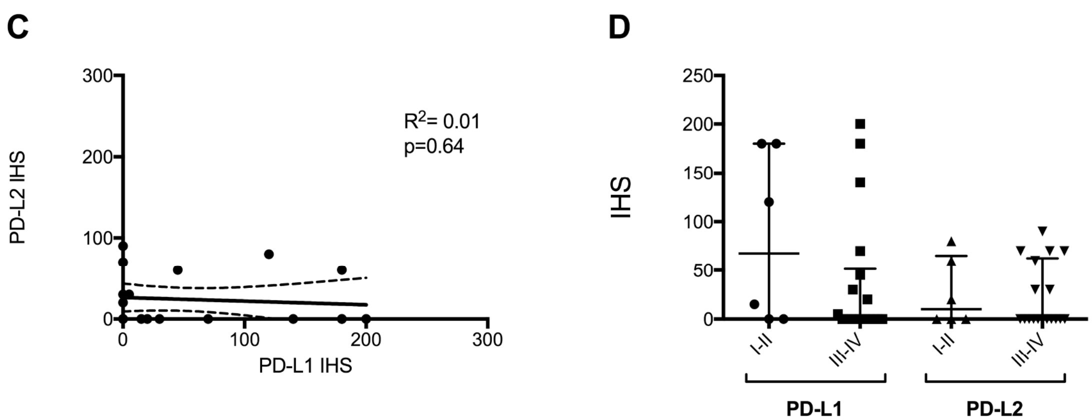

Panel C illustrates the relationship between PD-L1 and PD-L2 expression in HIV-associated NSCLC. **Panel D** illustrates the difference in PD-L1 and PD-L2 expression across the various TNM stages of NSCLC in HIV-associated NSCLC (n=24). Medians and interquartile ranges are reported.

E

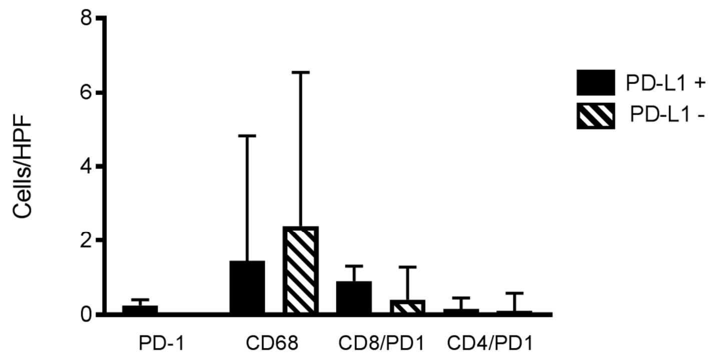

F

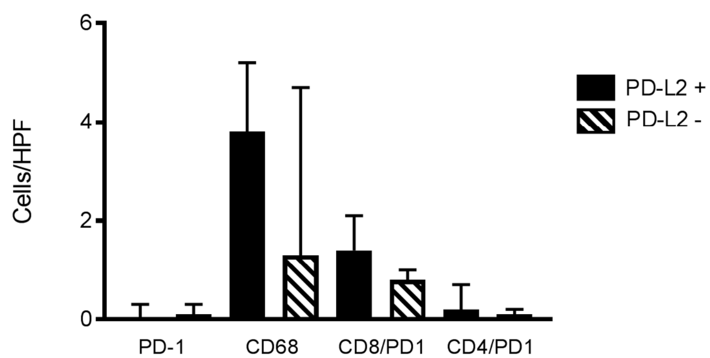

Panels E-F Histograms of multiplex immunohistochemistry experiments illustrating the relationship between PD-L1 (**Panel E**) and PD-L2 expression (**Panel F**) and the proportion of CD4, CD8, PD-1, CD68 or CD8/PD-1 and CD4/PD-1 immunopositive cells.

Figure S2.

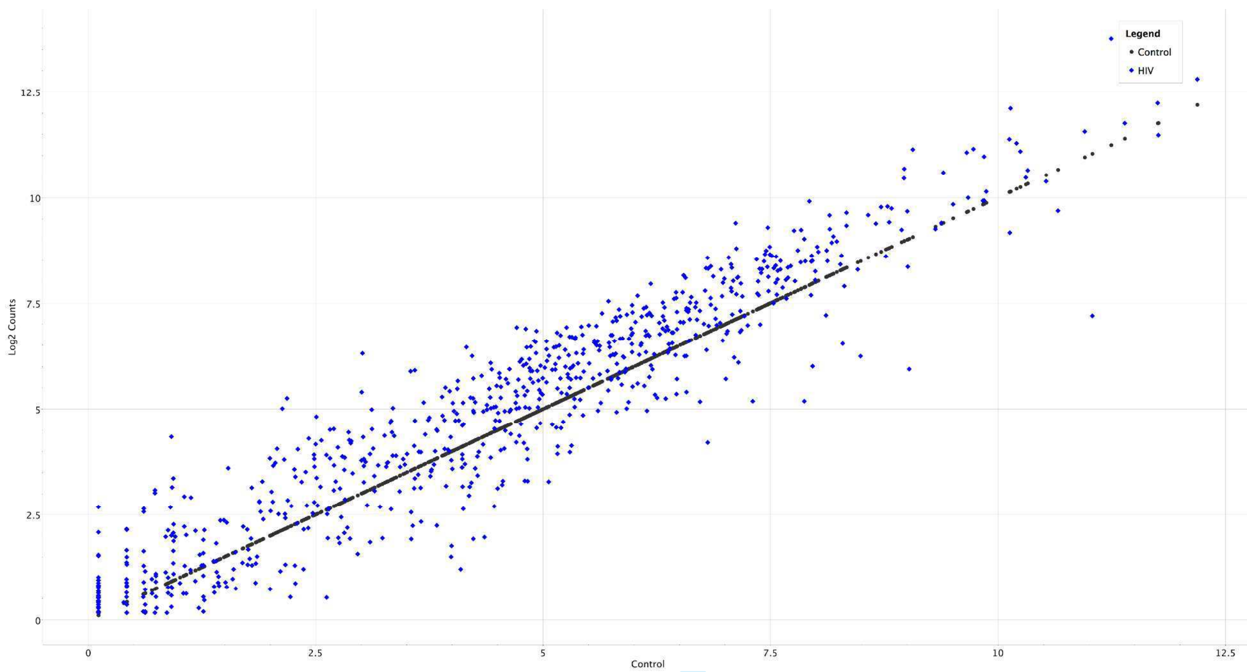

Scatter plot of the Nanostring transcriptomic analysis using the Nanostring PanCancer Immune panel. Each dot represents the average Log2 normalised read counts for each analysed transcript across two groups: HIV-associated NSCLC (n=5, blue) plotted against HIV-negative controls (n=3, black). The relative abundance of each transcript above (overexpression) or below the black line (underexpression) can be visually inferred to determine gene expression differences across cases versus controls. Gene expression was analysed using the Nsolver software (Version 4.0).

Figure S3.

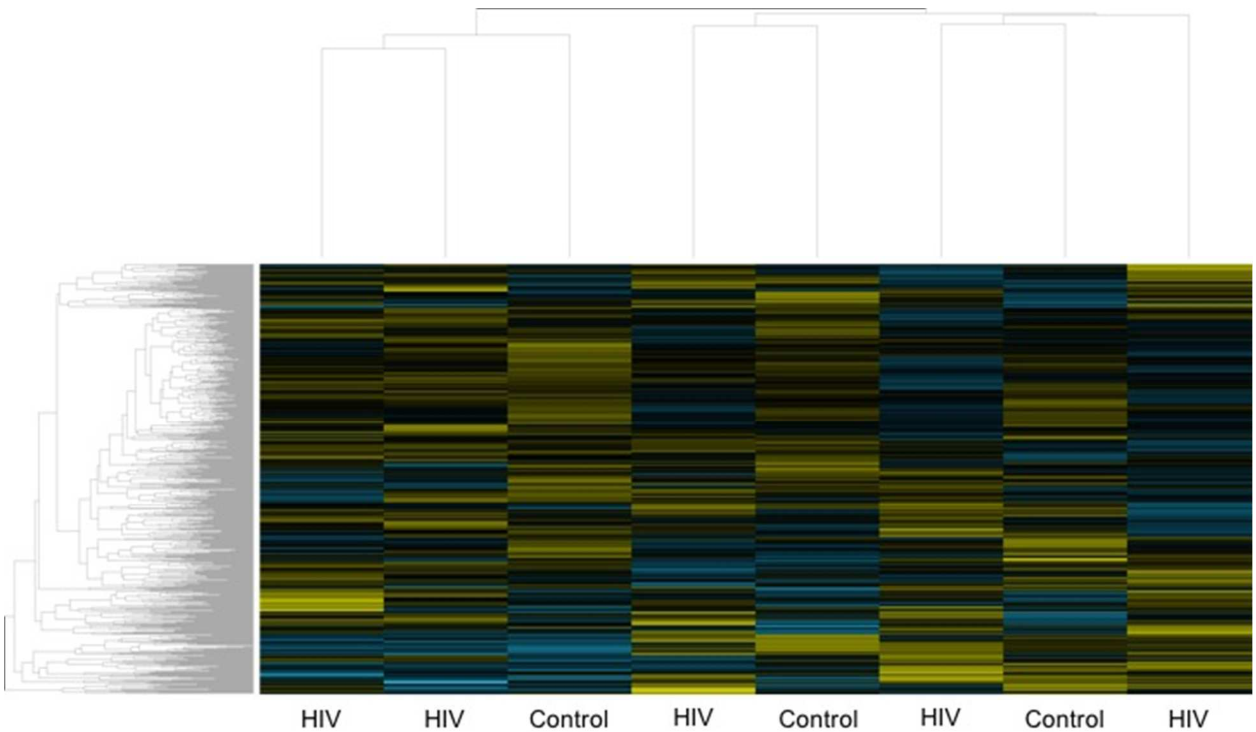

Heat map diagram of differential gene expression using Euclidean distance metrics in HIV-associated NSCLC compared to HIV-negative controls. Each column represents a patient and each row represents a single gene. Expression levels are coloured yellow for high intensities and green for low intensities.

<u>Table S1</u>.

Clinicopathologic features of the patient cohort.

Characteristic (%)	NSCLC (n=197)	HIV-associated NSCLC (n=24)
Age, median (IQR)	65 (13)	54 (11)
Gender		
Male	98 (50)	21 (87)
Female	98 (50)	3 (12)
TNM Stage		
I	110 (55)	4 (17)
II	57 (29)	2 (9)
III	24 (12)	7 (29)
IV	1 (1)	10 (45)
Missing	5 (2)	
Histological Subtype		
Adenocarcinoma	119 (60)	10 (42)
Squamous Cell Carcinoma	50 (25)	8 (37)
Others	28 (13)	5 (21)
Tumour Grade		
Well differentiated	38 (18)	0 (0)
Moderately differentiated	100 (50)	9 (37)
Poorly differentiated	60 (32)	14 (63)
CD4	-	
cell count (per µL)		432 (179)
%		27 (16)
CD8	-	
cell count (per µL)		809 (409)
%		48 (11)
CD19		
cell count (per µL)	-	196 (290)
%		11 (13)
CD56	-	
cell count (per µL)		129 (119)
%		7 (7)
CD4/CD8 ratio		
<0.4	-	4 (17)
0.4-1.0		17 (70)
>1.0		3 (13)

HIV RNA	-	
<50 copies/ml		5 (21)
>50 copies/ml		19 (79)
CDC HIV stage		
A1	-	5 (21)
A2		1 (4)
A3		2 (8)
B1		0 (0)
B2		2 (8)
B3		0 (0)
C1		2 (8)
C2		6 (30)
C3		5 (21)
Antiretroviral therapy at lung cancer diagnosis	-	
PI		13 (54)
NNRTI		12 (50)
II		1 (4)
NRTI		21 (87)
INI		1 (4)
Not on ARVs		2 (8)
Risk factor for HIV	-	
MSM contact		14 (63)
Heterosexual contact		7 (29)
Intravenous drug use		2 (8)
Duration of HIV infection in years, median (IQR)	-	16.6 (7)
Duration of HIV treatment in years, median (IQR)		9.8 (6)

Abbreviations:

CDC system: U.S. Centers for Disease Control and Prevention (CDC) classification system; ARV antiretrovirals, Protease Inhibitor (PI), Non-nuclease reverse transcriptase inhibitor (NNRTI), Integrase inhibitor (II), Nucleoside reverse transcriptase inhibitor (NRTI), MSM men who have sex with men.

Table S2.

Clinico-pathologic characteristics of patient samples undergoing targeted transcriptomic profiling using the Nanostring PanCancer Immune Panel.

Patient	Histotype	TNM Stage
HIV 1	Squamous cell carcinoma	I
HIV 2	Squamous cell carcinoma	I
HIV 3	Squamous cell carcinoma	II
HIV 4	Adenocarcinoma	II
HIV 5	Pleomorphic carcinoma	II
Control 1	Squamous cell carcinoma	I
Control 2	Squamous cell carcinoma	II
Control 3	Adenocarcinoma	II

Table S3.

Differentially regulated transcripts in HIV-associated NSCLC compared to HIV-negative controls.

Gene	p value	Fold Difference (HIV/control)	FDR q value
LAMP1	<0.00001	8.04	<0.00001
COL3A1	<0.00001	4.34	<0.00001
FN1	<0.00001	0.06	<0.00001
UBC	<0.00001	1.59	<0.00001
SPP1	<0.00001	3.54	<0.00001
FOS	<0.00001	3.67	<0.00001
HLA-DRA	<0.00001	2.74	<0.00001
HLA-A	0.00004	2.27	0.00349
APP	0.00004	2.89	0.0036
CCL18	0.00006	6.54	0.00437
RPS6	0.00012	1.41	0.00842
MUC1	0.00052	5.53	0.03311

Functional immune characterization of HIV-associated non-small cell lung cancer.

D.J. Pinato[1,2], A. Kythreotou[1], F. A. Mauri[1,3], E. Suardi[2], E. Allara[1,4], R. Shiner[5], A. U. Akarca[6], P. Trivedi[3], N. Gupta[3], A. D. Pria[2], T. Marafioti[6], P. Oliveri[7], T. Newsom-Davis[4], M. Bower[4]

1. Department of Surgery & Cancer, Imperial College London, Hammersmith Hospital, Du Cane Road, W120HS London, UK.

2. National Centre for HIV Malignancies, Chelsea & Westminster Hospital, SW10 9NH London (UK).

3. Department of Histopathology, Imperial College London, Hammersmith Hospital, Du Cane Road, W120HS London, UK.

4. NIHR Blood and Transplant Research Unit, Department of Public Health and Primary Care, University of Cambridge, UK

5. National Heart and Lung Division, Imperial College London (UK)

6. Department of Histopathology, University College London, 4th Floor Rockefeller Building, 21 University Street, London WC1E 6DE.

7. Department of Genetics, Evolution and Environment & Cell and Developmental Biology University College London Room 432, Darwin Building Gower Street, London, WC1E 6BT, UK

Word Count: 500 **Tables:** 0 **Figures:** 1

Running Head: *Immune characterisation of HIV-associated lung cancer*

To whom correspondence should be addressed:

Professor Mark Bower

E-mail: m.bower@imperial.ac.uk

Letter to the Editor.

Dear Editor,

In the combined anti-retroviral therapy (cART) era, non-small cell lung cancer (NSCLC) is a highly incident cause of morbidity and mortality in people living with HIV (PLHIV)[1]. The immune-pathogenesis of NSCLC and HIV infection both rely on programmed-death 1 (PD-1) receptor-ligand interaction as a mechanism to induce T-cell exhaustion. To date, PLHIV have been excluded from clinical trials of immune-checkpoint inhibitors (ICPI), on the presumption that anti-tumour immunity might be compromised by HIV infection. To verify this, we evaluated the clinico-pathologic significance of PD-ligands expression in a consecutive series of 221 archival NSCLC samples, 24 of which were HIV-associated (**Table S1**).

Most patients with HIV-associated NSCLC were active smokers (*n*=18, 75%; median 40 packs/year, IQR 48), established on cART (*n*=22, 92%) for a median duration of 9.7 years (IQR 7.1) with CD4 counts >250 cells/mm^3 (*n=19*, 79%) and suppressed HIV RNA (*n*=20, 80%). Molecular profiling data (*n*=12/24) revealed two EGFR mutation carriers. Tissue-microarray sections underwent PD-L1, PD-L2 immunostaining and multiplex immunohistochemistry (*n*=21) for PD-1, CD4, CD8 and CD68 (**Figures 1A-D, Supplementary Materials**). Prevalence of PD-L1 positivity was

45% in tumour (*n*=11/24) and 8% (*n*=2/24) in tumour-infiltrating cells, whereas tumoural PD-L2 positivity was found in 33% (*n*=8/24) (**Figure S1)**. Following 2:1 case-control matching for age, gender, grade, stage and histotype (*n*=66), PD-L1 (12/23 vs 14/43, p=0.12) and PD-L2 expression (9/23 vs 25/45, p=0.20) were unrelated to the presence and severity of HIV-related immune dysfunction as indicated by nadir CD4 counts (p=1.0, p=0.8), HIV RNA levels (p=0.14, p=0.24), duration of HIV infection and cART (p>0.05) suggesting independence between anti-viral and anti-tumour immune-tolerogenesis. In keeping with this view, we documented a positive correlation between PD-L1 expression and density of tumour-infiltrating (TIL) (**Figure 1A-F**) but not peripherally circulating lymphocytes (**Figure 1G-H**), highlighting polarization of the tumour microenviroment to a type-1 response[2]. In type-1 or PD-L1^{+}/TIL^{+} tumours, TILs are chemo-attracted to malignant cells and turned off by PD-L1 engagement. Type-1 tumours are generally sensitive to single-agent PD-1/PD-L1-targeted checkpoint blockade, due to the presence of an immune-reactive microenvironment[3].

In an exploratory targeted transcriptomic analysis of 5 HIV-positive cases and 3 stage/histotype-matched controls using the NanoString PanCancer-Immune panel (NanoString Technologies, Seattle, USA), we demonstrated enrichment of transcripts involved in chemotaxis (CCL18), antigen presentation (HLA-A, HLA-DRA), cytotoxic T-cell (LAMP-1) and macrophage activation (SPP1, **Figure 1I-L**) in HIV-associated NSCLC, consistent with previous studies[4]. Whilst not exhaustive and limited by sample size, our findings challenge the conception that well-controlled HIV infection may negatively influence cancer-specific immune dysfunction by preliminarily demonstrating the presence of an immune-reactive microenvironment in HIV-associated

NSCLC (**Figure S2-3, Table S2-3**). This concept should be further explored by comparing normal and neoplastic lung tissues in prospective studies.

As accumulating evidence shows PD-1/PD-L1-targeted ICPI to be safe and capable of enhancing HIV-specific immunity[5] without unexpected toxicity, taken together, our data suggest that HIV-associated NSCLC may be equally reactive to ICPI. Whilst preliminary in nature and warranting validation in larger patient cohorts treated with ICPI, our study supports an immunobiologic rationale for the development of PD-1/PD-L1-targeted ICPI in HIV-associated NSCLC.

References.

1. Bower M, Powles T, Nelson M et al. HIV-related lung cancer in the era of highly active antiretroviral therapy. AIDS 2003; 17: 371-375.

2. Teng MW, Ngiow SF, Ribas A, Smyth MJ. Classifying Cancers Based on T-cell Infiltration and PD-L1. Cancer Res 2015; 75: 2139-2145.

3. Taube JM, Klein A, Brahmer JR et al. Association of PD-1, PD-1 ligands, and other features of the tumor immune microenvironment with response to anti-PD-1 therapy. Clin Cancer Res 2014; 20: 5064-5074.

4. Domblides C, Antoine M, Hamard C et al. Non-small cell lung cancer from HIV-infected patients expressed PD-L1 with marked inflammatory infiltrates. AIDS 2017.

5. Guihot A, Marcelin AG, Massiani MA et al. Drastic decrease of the HIV reservoir in a patient treated with nivolumab for lung cancer. Ann Oncol 2017.

Figure Legends.

Figure 1. Panel A-D. Representative sections of HIV-associated NSCLC co-immunostained for CD8 (red chromogen), CD4 (brown chromogen), PD-1 (blue chromogen) and CD68 (green chromogen) illustrating CD4/CD8 enrichment in PD-L1-positive HIV-associated NSCLC (**Panels A-C**) compared to PD-L1-negative counterparts (**Panels B-D**). **Panels E-F** Histograms of multiplex immunohistochemistry data illustrating the relationship between the CD4 and CD8-positive immune infiltrate expressed as number of immunopositive cells per high power field (HPF) according to tumour cell PD-L1 (**Panel E**) and PD-L2 expression status (**Panel F**) in HIV-associated NSCLC (*n*=21). **Panels G-H** Peripheral blood immunophenotyping illustrates the relationship between peripheral CD4, CD8, CD19 and CD56-positive cell counts categorized according to tumoural PD-L1 (**Panel G**) and PD-L2 expression status (**Panel H**) in HIV-associated NSCLC (*n*=24). Medians and interquartile ranges are reported. **Panel I:** Volcano plot of differentially-regulated genes identified by Nanostring analysis. The Benjamini-Hockberg p-values are correlated to fold-changes in transcripts identified in HIV-positive NSCLC (*n*=5) versus HIV-negative controls (*n*=3). Transcripts achieving statistical significance (FDR q-value of 5%) are highlighted by the presence of the corresponding gene name. **Panel L.** Heat map profile of the 12 transcripts that are differentially regulated in HIV-associated NSCLC compared to controls. Expression levels are shown as log transformed values of normalized counts (ln2).

Conflict of interest: None declared.

Acknowledgements.

The authors would like to acknowledge the Imperial College Healthcare NHS Trust Tissue Bank for having supported the study.

Funding

DJP is supported by grant funding from the National Institute for Health Research (NIHR), the Imperial Biomedical Research Centre and the Academy of Medical Sciences (AMS Grant ID SGL013/1021). The AMS Starter Grant is jointly funded by the AMS, Wellcome Trust, Medical Research Council, British Heart Foundation, Arthritis Research UK, the Royal College of Physicians and Diabetes UK.